2018 26th Mediterranean Conference on Control and Automation (MED)
Zadar, Croatia, June 19-22, 2018

# Sliding Mode Control of Launch Vehicles' Flight Path Slope Angle

Romulus Lungu, Florentin Alin Buţu, and Mihai Lungu

*Abstract*— **The paper presents the design of an adaptive system for the control of flight path slope angle associated to launch vehicles' motion in vertical plane during their second flight stage, after the launch phase, by using the sliding mode control and the dynamic inversion principle. The control law is obtained by means of a Lyapunov positive defined function and it is based on the estimation of an unknown aerodynamic parameters. The theoretical results are validated in Matlab for a concrete example associated to a launch vehicle's motion in vertical plane.**

***Keywords — launch vehicle; dynamic inversion; sliding mode control; path slope angle.***

## I. Introduction

The spaceflight facilitates the observation of the different phenomena occurring on Earth, as well as space exploration and the launching of communication satellites or space telescopes; also, it can be the solution to major problems such as the overpopulation of Earth or the scarce natural resources [1]. To transport a space vehicle (capsule, satellite etc.) into space, a carrier rocket (launch vehicle) is needed; the part of the trajectory from the launch point to the point where the payload is placed into orbit is called the active segment of the trajectory [1]. Considering the launching phase as the first flight stage for a launch vehicle, during the second flight stage, the payload (remained after the removal of the launch vehicle's first steps) should be inserted into a transition or final orbit. The payload represents the module (satellite, capsule etc.) that later becomes the space vehicle.

In the literature there are some papers dealing with the control of launch vehicles' motion in vertical plane [1-11]. Having in mind that the launch vehicles are subject to poor flight conditions, severe parameter uncertainties or unknown external disturbances [2, 3], their attitude and trajectory control is still a challenging problem. In this purpose, the gain scheduling control was used in [4]; although this method generally solves the control issues, the robustness and global stability of the system cannot be guaranteed in the case of large variation of the control parameters. In [5], the trajectory linearization control was used to improve the nonlinear performances in flight control system for aircrafts, but the main weakness is the finite robust performance because of the linearized dynamics. The use only of the dynamic inversion method did not cope with the flight control problem of a reusable launch vehicle in [6], the drawback of this control technique being the poor robustness in the case of severe parameter uncertainties and modeling errors; this is why, in the present paper, as an innovative element, the dynamic inversion technique is used together with the sliding mode control which is well known as a robust method to design control law for uncertain system [7]. In [8], a robust control approach was used to tackle the flight control in presence of hard constraints, model uncertainties, and external disturbances, the main drawback being that the robust control architecture cannot achieve a good tracking performance because the robust controller is designed in the worst case of the control system. In [9], a new adaptive sliding mode attitude controller is designed for a rocket's dynamics incorporating faults and unknown disturbances; the weakness of the controller is that the boundary values of the uncertainties and disturbances should be completely known, requirement hard to satisfy in practical experiments. To improve the tracking control performance of the flight control systems, the fuzzy logic control has been combined with other control techniques, e.g. the robust control [10] or the H-infinity control method [11].

By using the vertical plane dynamics of the launch vehicles with respect to Earth [12], in the present paper, there is designed a new adaptive system for the flight path slope angle control by using the dynamic inversion technique [13] and the sliding mode control [14]. Generally, by using the sliding mode control (SMC – nonlinear control approach characterized by robustness, accuracy, and easy tuning and implementation), the states are driven onto a particular surface in the state space (sliding surface). After the reach of this surface, the states are kept on the close neighborhood of this sliding surface by the SMC. The SMC firstly considers the design of a sliding surface such that the design specifications are satisfied by the sliding motion; then, there is selected the control law that will make the switching surface attractive to the system states [15]. The design of the new adaptive control system involves the deduction of the relative degree associated to the rocket's dynamics with respect to flight path slope angle [16]. The reference model of the adaptive control system is chosen as a three-order reference model; its input is the calculated slope angle $\gamma_c$ computed as in [17]. Another innovative element is related to the control law which depends on the estimated aerodynamic parameters for the launch vehicle's dynamics. One chooses a nonlinear Lyapunov function [18, 19] and, from the condition providing that the adaptive control system is stable [20-22], one deduces the equations of the estimated variables depending on the estimated aerodynamic parameters. The control law is designed with respect to these estimated parameters. For the designed control architecture's validation, it is software implemented in Matlab and the time characteristics associated to the launch vehicle's dynamics are obtained.

This work is supported by a grant of the Romanian National Authority for Scientific Research and Innovation, CNCS/CCCDI – UEFISCDI, project code PN-III-P2-2.1-PED-2016-0395, within PNCDI III

Romulus Lungu is with University of Craiova, Faculty of Electrical Engineering, Craiova, Romania (e-mail: romulus_lungu@yahoo.com).

Florentin Alin Buţu is with University "Politehnica" of Bucharest, Faculty of Aerospace Engineering, Romania (e-mail: florentinalin@yahoo.com).

Mihai Lungu is with University of Craiova, Faculty of Electrical Engineering, Craiova, Romania (e-mail: Lma1312@yahoo.com).

## II. Launch Vehicle's Dynamics in Vertical Plane

During the launching phase, the first step of the rocket is detached after about 126 seconds, while the second step of the rocket is detached after another 157 seconds; only the rocket module (satellite, capsule etc.) remains; its flight slope angle should be controlled during the second flight stage (before the insert of the module into an orbit).

In Fig. 1 the forces acting on the rocket are highlighted in the second stage of flight; $R_p$ is the radius of Earth, $H$ – the flight altitude, $\theta$ – the pitch angle, $\vartheta$ and $d$ – the angle and the distance travelled during the second flight stage, respectively. The used forces are: $\vec{G}$ – the gravity force ($\vec{G} = -K_p \frac{\vec{r}}{r^3}$, $\vec{r}$ – the position vector of the launch vehicle with respect to the Earth center, $r = R_p + H$, $K_p$ – the gravitational constant of Earth, $K_p = \chi m_p$, $\chi$ – the universal gravity constant, $m_p$ – the mass of Earth), $\vec{L}$ – the lift force, $\vec{D}$ – the drag force, $\vec{F}_c$ – the thrust force of the launch vehicle, $\vec{F}_f$ – the centrifugal force, while $\vec{F}_i = -m\vec{a} = -m\dot{\vec{V}}$ is the inertia force of the rocket; $\vec{a} = \dot{\vec{V}}$ is the launch vehicle's acceleration, while $m$ is its mass.

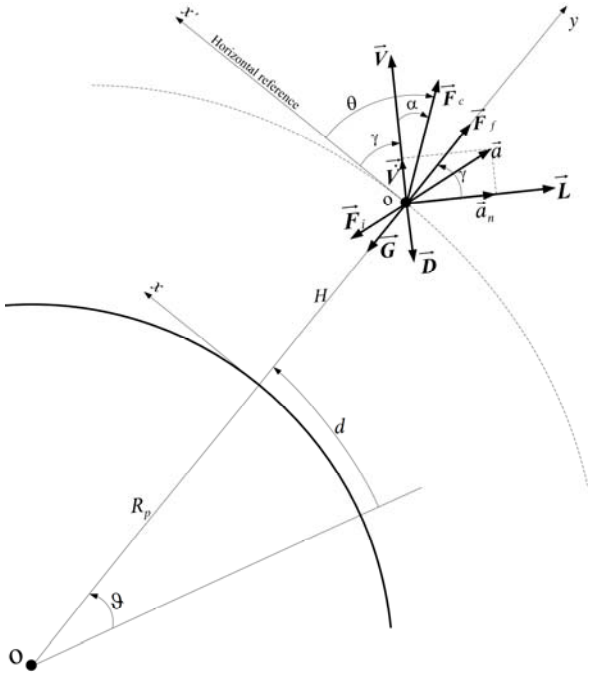


Fig. 1. Forces acting on the launch vehicle during the second flight phase

The dynamics of the rocket (considered as a material point) is described by the equilibrium equation of the forces:

$$\vec{F}_c + \vec{G} + \vec{L} + \vec{D} + \vec{F}_f + \vec{F}_i = 0, \tag{1}$$

equivalent with:

$$\begin{aligned} m\left(\dot{\vec{V}} + \dot{\vec{\gamma}} \times \vec{V}\right) &= \vec{F}_c + \vec{G} + \vec{L} + \vec{D} + \vec{F}_f, \\ \vec{a} = \dot{\vec{V}} &= \vec{V} + \vec{a}_n = \dot{\vec{V}} + \dot{\vec{\gamma}} \times \vec{V}. \end{aligned} \tag{2}$$

Projecting the first equation (2) on the directions of the axes associated to the velocity $\vec{V}$ and on its normal axis, by neglecting the component of the centrifugal force, one gets:

$$\begin{aligned} \dot{V} &= \frac{1}{m} F_c \cos\alpha - k\frac{\sin\gamma}{r^2} - \frac{D}{m}, \\ \dot{\gamma} &= \frac{1}{mV} F_c \sin\alpha - k\frac{\cos\gamma}{r^2 V} + \frac{L}{mV} + \frac{V\cos\gamma}{r}; \end{aligned} \tag{3}$$

one denoted: $k = K_p / m = g\, r^2$ ($g$ – the gravity acceleration).

The tangential component of the velocity $\vec{V}$ generates a rotation with the angular rate:

$$\dot{\vartheta} = \frac{V\cos\gamma}{r}. \tag{4}$$

The radial component of velocity $\vec{V}$ leads to the modification of the flight altitude $H$ (i.e. of the rocket's position vector $r$ with respect to the center of Earth) with the speed:

$$\dot{H} = \dot{r} = V\sin\gamma. \tag{5}$$

The variation velocity of the fuel mass, and, thus, of the rocket's mass, is expressed by the equation:

$$\dot{m} = -\frac{F_c}{c}, c = g_0 c', \tag{6}$$

where $c$ is the specific impulse of the exhaust gas mass ($c = mV_g / m = V_g$ – the speed of the gas), while $g_0$ is the gravity acceleration at altitude $H$=0.

The obtaining of other equations which describes the launch vehicle's dynamics can be done by using two inertial frames: $oxyz$ – body-fixed reference frame (with the origin in the vehicle's center of mass, $ox$ – the longitudinal axis, $oy$ – the right oriented axis, $oz$ – the axis perpendicular to the plane $oxy$) and $o_g x_g y_g z_g$ – the reaction nozzle tied inertial frame (the reaction nozzle is mounted together with the reaction engine in cardanic suspension). The position of point $o_g$ with respect to point $o$ is described along the axis $ox$ by $r_{gx}$. Considering $T$ – the thrust force of the reaction nozzle and $\delta$ – the reaction nozzle's rotation angle, the equilibrium equations of the moments acting around the axis $oy$ are:

$$\begin{aligned} J_{yy}\dot{\omega}_y &= M_y, M_y = M_{ay} + M_{cy}, \\ M_{ay} &= QS\left(bC_y + r_{px}c_z\right), M_{cy} = -Tr_{gx}\delta, \end{aligned} \tag{7}$$

with $J_{yy}$ – the inertia moment with respect to axis $oy$, $M_{ay}$ – the aerodynamic moment, $M_{cy}$ – the command moment around the axis $oy$, $\omega_y$ – the angular rate with respect to axis $oy$, $C_y = c_y^{\alpha}\alpha$ – the coefficient of the aerodynamic moment $M_{ay}$, $\alpha$ – the attack angle of the rocket, and $c_z$ – the coefficient of the rocket's lift force having its origin at the distance $r_{px}$ from the launch vehicle's centre of mass. The angular rate $\omega_y$ is expressed as the time derivative of the pitch angle $\theta$:

$$\dot{\theta} = \omega_y, \theta = \gamma + \alpha. \tag{8}$$

According to Fig. 1, $\gamma$ is the flight path slope angle; from equations (7), one obtains:

$$\dot{\omega}_y = \frac{QS}{J_{yy}}\left(r_{p_x} c_z + bC_y\right) - Tr_{gx}\delta. \tag{9}$$

Concluding, the launch vehicles' dynamics in vertical plane is described by Eqs. (3), (4), (6), (8), and (9), i.e. the equations associated to rocket's velocity ($\boldsymbol{V}$), position vector with respect to the centre of Earth ($\boldsymbol{r}$), mass of the rocket ($m$), rotation angle of the launch vehicle with respect to Earth $(\vartheta)$, flight path slope angle $(\gamma)$, angular rate $(\omega_y)$, and pitch angle $(\theta)$:

$$\begin{aligned}
&\dot{\boldsymbol{V}} = \frac{1}{m}\boldsymbol{F}_c\cos\alpha - \frac{\boldsymbol{D}}{m} - \frac{K_p \sin\gamma}{m\boldsymbol{r}^2},\ \boldsymbol{D} = QSc_x,\ Q = \rho\frac{\boldsymbol{V}^2}{2},\\
&\dot{\boldsymbol{r}} = \boldsymbol{V}\sin\gamma,\\
&\dot{m} = -\frac{\boldsymbol{F}_c}{c},\\
&\dot{\vartheta} = \frac{\boldsymbol{V}\cos\gamma}{\boldsymbol{r}},\\
&\dot{\gamma} = \frac{1}{m\boldsymbol{V}}\boldsymbol{F}_c\sin\alpha + \frac{\boldsymbol{L}}{m\boldsymbol{V}} - \frac{K_p\cos\gamma}{m\boldsymbol{r}^2\boldsymbol{V}} + \frac{\boldsymbol{V}\cos\gamma}{\boldsymbol{r}},\ \boldsymbol{L} = QSc_z,\\
&\dot{\omega}_y = \frac{QS}{J_{yy}}\left(r_{p_x}c_z + bC_y\right) - Tr_{gx}\delta,\ c_z = c_{z_0} + c_z^{\alpha}\alpha, C_y = c_y^{\alpha}\alpha,\\
&\dot{\theta} = \omega_y,\ \alpha = \theta - \gamma.
\end{aligned} \tag{10}$$

The last three equations (10), considering the state vector $\boldsymbol{x} = \begin{bmatrix}\gamma & \omega_y & \theta\end{bmatrix}^{\mathrm{T}}$ and the input $u = \delta$, lead to the state equation:

$$\dot{\boldsymbol{x}} = \boldsymbol{f(x)} + Bu, \tag{11}$$

where

$$\boldsymbol{f}(\boldsymbol{x}) = \begin{bmatrix} a_{11}\cos\gamma + a_{12}(\theta-\gamma) + a_{13} \\ a_{21}(\theta-\gamma) + a_{22} \\ \omega_y \end{bmatrix},\ B = \begin{bmatrix} 0 \\ b \\ 0 \end{bmatrix}, \tag{12}$$

with

$$\begin{aligned}
&a_{11} = -\frac{K_p}{m\boldsymbol{r}^2\boldsymbol{V}} + \frac{\boldsymbol{V}}{\boldsymbol{r}} = -\frac{g}{\boldsymbol{V}} + \frac{\boldsymbol{V}}{\boldsymbol{r}},\ a_{12} = \frac{F_c}{m\boldsymbol{V}} + \frac{\rho\boldsymbol{V}S}{2m}c_z^{\alpha},\\
&a_{13} = \frac{\rho\boldsymbol{V}S}{2m}c_{z_0},\ a_{21} = \frac{\rho\boldsymbol{V}^2 S}{2J_{yy}}\left(r_{px}c_z^{\alpha} + bc_y^{\alpha}\right),\\
&a_{22} = \frac{\rho\boldsymbol{V}^2 S}{2J_{yy}}r_{px}c_{z_0},\ b = -Tr_{gx}\frac{\rho\boldsymbol{V}^2 S}{2J_{yy}}.
\end{aligned} \tag{13}$$

## III. Design of the Adaptive Control System

The first step of the adaptive control system design is to deduce the relative degree ($r$) associated to the launch vehicle's dynamics with respect to flight path slope angle $(\gamma)$; for this, the output $y = \gamma$ is derived so many times until the command variable $u = \delta$ appears in the $r$-order derivative $y^{(r)}$ [13]; it is easy to obtain $r = 3$, since the next equation resulted:

$$\dddot{y} = \dddot{\gamma} = f_0 + a_{12}f_1 + a_{12}^2 f_2 + a_{12}(a_{12}^2 + a_{21})f_3 + a_{12}bu, \tag{14}$$

where $f_i, i = \overline{0,3}$, are nonlinear functions (depending on the states of the system) having the qualitative forms [18]:

$$\begin{aligned}
&f_0 = a_{11}^2 a_{13}\left(\cos^2\gamma + \cos 2\gamma\right) - a_{11}a_{13}^2\cos\gamma - a_{11}^3\cos\gamma\cos 2\gamma = f_0(\gamma),\\
&f_1 = -a_{11}^2\left(\cos^2\gamma + \cos 2\gamma\right)f_3 + a_{11}^2\sin 2\gamma - 2a_{11}a_{13}f_3\cos\gamma +\\
&\quad + a_{11}\left(2a_{13} - \omega_y\right)\sin\gamma = f_1(\gamma, \omega_y, \theta),\\
&f_2 = 2a_{11}f_3\sin\gamma - a_{11}f_3^2\cos\gamma + a_{11}\cos\gamma - \omega_y + a_{13} = f_2(\gamma, \omega_y, \theta),\\
&f_3 = \theta - \gamma = \alpha = f_3(\gamma, \theta).
\end{aligned} \tag{15}$$

The command variable $u$ can be expressed from equation (14) as follows:

$$u = \delta = g\left(\dddot{\gamma} - f_0\right) + \sum_{i=1}^{3}\lambda_i f_i, \tag{16}$$

with

$$g = \frac{1}{a_{12}b}, \lambda_1 = -\frac{1}{b}, \lambda_2 = -\frac{a_{12}}{b}, \lambda_3 = -\frac{a_{12}^2 + a_{21}}{b}. \tag{17}$$

One designs the control law:

$$\hat{\sigma} = \hat{h}_r(y, \hat{u}) = \hat{h}_r(\gamma, \hat{\delta}), \tag{18}$$

where $\hat{h}_r$ represents the best approximation of the function $\sigma = y^{(r)} = h_r(y,u)$; also, $\varepsilon = h_r(y,u) - \hat{h}_r(y,\hat{u})$ is the inversion (approximation) error of the function $h_r$, which acts as a disturbance. The inverses of the functions $\sigma$ and $\varepsilon$ are [12]:

$$\begin{aligned}
&\hat{u} = \hat{\delta} = \hat{h}_r^{-1}(y, \hat{\sigma}) = \hat{h}_r^{-1}(\gamma, \hat{\sigma}),\\
&u = \delta = h_r^{-1}(y, \sigma) = h_r^{-1}(\gamma, \sigma).
\end{aligned} \tag{19}$$

The function $\varepsilon$ has the form of the second equation (19), i.e.:

$$\begin{aligned}
&h_r^{-1}(y, \sigma) = h_r^{-1}(\gamma, \sigma) = g\left(\dddot{\gamma} - f_0\right) + \sum_{i=1}^{3}\lambda_i f_i,\\
&\hat{h}_r^{-1}(y, \hat{\sigma}) = h_r^{-1}(\gamma, \hat{\sigma}) = \hat{g}\left(\dddot{\gamma} - \hat{f}_0\right) + \sum_{i=1}^{3}\hat{\lambda}_i f_i,
\end{aligned} \tag{20}$$

where $\hat{g}$ and $\hat{\lambda}_i$ represent the estimates of the unknown parameters $g$ and $\lambda_i, i = \overline{0,3}$, respectively.

Developing the function $u = h_r^{-1}(y, \sigma)$ in Taylor series around the pair of variables $(y, \hat{\sigma})$, it results:

$$\begin{aligned}
u &\cong h_r^{-1}(y,\sigma) = \hat{h}_r^{-1}(y,\sigma) + \frac{\mathrm{d}}{\mathrm{d}\sigma}\left(h_r^{-1}(y,\sigma)\right)_{\sigma=\hat{\sigma}}\left(\sigma - \hat{\sigma}\right) =\\
&= \hat{h}_r^{-1}(y,\hat{\sigma}) + \frac{\mathrm{d}}{\mathrm{d}\hat{\sigma}}\left(\hat{h}_r^{-1}(y,\hat{\sigma})\right)\varepsilon = \hat{u} + \frac{\mathrm{d}}{\mathrm{d}\hat{\sigma}}\left(\hat{h}_r^{-1}(y,\hat{\sigma})\right)\varepsilon.
\end{aligned} \tag{21}$$

From equation $\varepsilon = h_r(y,u) - \hat{h}_r(y,\hat{u})$, one obtains:

$$\sigma = \ddot{y} = \dddot{\gamma} = h_r(\gamma, \delta) = \frac{1}{g}\left[\left(\delta + gf_0\right) - \sum_{i=1}^{3}\lambda_i f_i\right]. \tag{22}$$

For stability analysis, one considers the Lyapunov function [23]: $V_1 = \frac{1}{2}\sigma^2$, with $\sigma = \ddot{e} + k_2\dot{e} + k_1 e, e = \gamma_d - \gamma$, and $k_1, k_2 -$

positive constants; in order to compute the derivative of the Lyapunov function, one firstly derivates the function $\sigma$ as:

$$\dot{\sigma}=\dddot{e}+k_2\ddot{e}+k_1\dot{e}=\dddot{\gamma}_d-\dddot{\gamma}+k_2\ddot{e}+k_1\dot{e}\overset{(22)}{=}\dddot{\gamma}_d+k_2\ddot{e}+k_1\dot{e}-$$
$$-\frac{1}{g}\left[\left(\delta+gf_0\right)-\sum_{i=1}^{3}\lambda_i f_i\right]=h-\frac{1}{g}\left[\left(\delta+gf_0\right)-\sum_{i=1}^{3}\lambda_i f_i\right], \quad (23)$$
$$h=\dddot{\gamma}_d+k_2\ddot{e}+k_1\dot{e},$$

and

$$\dot{V}_1=\sigma\cdot\dot{\sigma}=\sigma\left\{\dddot{\gamma}_d+k_2\ddot{e}+k_1\dot{e}-\frac{1}{g}\left[\left(\delta+gf_0\right)-\sum_{i=1}^{3}\lambda_i f_i\right]\right\}=$$
$$=\sigma\left\{h-\frac{1}{g}\left[\left(\delta+gf_0\right)-\sum_{i=1}^{3}\lambda_i f_i\right]\right\}. \quad (24)$$

One chooses:

$$\delta=h_r^{-1}(\gamma,\sigma)=g\left[\left(\dddot{\gamma}_d+k_2\ddot{e}+k_1\dot{e}\right)-f_0\right]+\sum_{i=1}^{3}\lambda_i f_i+k\sigma=$$
$$=g\left(h-f_0\right)+\sum_{i=1}^{3}\lambda_i f_i+k\sigma. \quad (25)$$

The function $f_0$ is calculated by means of equation (15), where $a_{11}$ and $a_{13}$ are obtained by using equations (13). Because $g$ and $\lambda_i, i=\overline{0,3}$, are unknown parameters, their estimated values ($\hat{g}$ and $\hat{\lambda}_i$) will be used; according to Eq. (25), it yields:

$$\hat{\delta}=\hat{h}_r^{-1}(\gamma,\sigma)=\hat{g}\left(\dddot{\gamma}_d+k_2\ddot{e}+k_1\dot{e}-f_0\right)+\sum_{i=1}^{3}\hat{\lambda}_i f_i+k\sigma=$$
$$=\hat{g}\left(h-f_0\right)+\sum_{i=1}^{3}\hat{\lambda}_i f_i+k\sigma. \quad (26)$$

Using Eq. (25), the expression of $\dot{\sigma}$ (Eq. (23)) becomes: $\dot{\sigma}=-\frac{k}{g}\sigma$; $\sigma$ converges asymptotically to zero and one gets: $g\dot{\sigma}+k\sigma=0$ and $\dot{V}_1=-\frac{k}{g}\sigma^2<0$ if and only if $g>0$. Since this condition is not always fulfilled, another Lyapunov function is chosen [18]:

$$V_2\left(\sigma,\tilde{g},\tilde{\lambda}_i\right)=\frac{1}{2}|g|\sigma^2+\frac{1}{2\eta}\left(\tilde{g}^2+\sum_{i=1}^{3}\tilde{\lambda}_i^2\right), \quad (27)$$

with $\tilde{g}=\hat{g}-g, \tilde{\lambda}_i=\hat{\lambda}_i-\lambda_i, \eta>0$. Because the function $g$ is unknown, $|g|$ is replaced by $|\hat{g}|$ in (27), one should choose $\dot{\hat{g}}$ and $\dot{\hat{\lambda}}_i$ such that the closed loop system is asymptotically stable, i.e. $\dot{V}_2\left(\sigma,\tilde{g},\tilde{\lambda}_i\right)\le 0$. By time derivation of Eq. (27), it results:

$$\dot{V}_2(\sigma,\tilde{g},\tilde{\lambda}_i)=|g|\sigma\dot{\sigma}+\frac{1}{\eta}\left(\tilde{g}\dot{\tilde{g}}+\sum_{i=1}^{3}\tilde{\lambda}_i\dot{\tilde{\lambda}}_i\right). \quad (28)$$

Because $g$ and $\lambda_i$ are slowly varying in time $\left(\dot{g}=\dot{\lambda}_i=0\right)$, one gets: $\dot{\tilde{g}}=\dot{\hat{g}}, \dot{\tilde{\lambda}}_i=\dot{\hat{\lambda}}_i, i=\overline{0,3}$. Replacing $\delta\cong\hat{\delta}$ with the form (26) into Eq. (23), one obtains:

$$\dot{\sigma}=h-\frac{1}{g}\left(\delta+gf_0\right)+\frac{1}{g}\sum_{i=1}^{3}\lambda_i f_i+k\sigma=$$
$$=-\frac{1}{g}\left[\tilde{g}\left(h-f_0\right)+\sum_{i=1}^{3}\tilde{\lambda}_i f_i+k\sigma\right], \quad (29)$$

and, with this, the equation (28) gets the form:

$$\dot{V}_2\left(\sigma,\tilde{g},\tilde{\lambda}_i\right)=-\frac{|g|}{g}\sigma\left[\tilde{g}\left(h-f_0\right)+\sum_{i=1}^{3}\tilde{\lambda}_i f_i+k\sigma\right]+$$
$$+\frac{1}{\eta}\left(\tilde{g}\dot{\tilde{g}}+\sum_{i=1}^{3}\tilde{\lambda}_i\dot{\tilde{\lambda}}_i\right)=\tilde{g}\left[-\frac{|g|}{g}\sigma\left(h-f_0\right)+\frac{1}{\eta}\dot{\tilde{g}}\right]+ \quad (30)$$
$$+\sum_{i=1}^{3}\left[-\frac{|g|}{g}\sigma f_i+\frac{1}{\eta}\dot{\tilde{\lambda}}_i\right]\tilde{\lambda}_i-\frac{|g|}{g}k\sigma^2.$$

Choosing

$$\dot{\hat{g}}=\eta(\operatorname{sgn}g)\sigma(h-f_0), \dot{\hat{\lambda}}_i=\eta(\operatorname{sgn}g)\sigma f_i, i=\overline{1,3}, \quad (31)$$

it results: $\dot{V}_2<0$, i.e. the closed loop system is asymptotically stable.

## IV. Structure of the New Adaptive Control Architecture and its Software Implementation

The block diagram of the adaptive system for the path slope angle control associated to launch vehicles' motion in vertical plane during their second flight stage after the launch phase by using the SMC and the dynamic inversion principle is presented in Fig. 2; it has been obtained by means of the equations given in the previous section.

For the calculation of the variables $\dot{\gamma}_d, \ddot{\gamma}_d, \dddot{\gamma}_d$, a three-order reference model is considered; its order is equal with the system relative degree ($r$=3) with respect to the slope angle $\gamma$; the reference model is described by the equation:

$$\frac{\gamma_d(s)}{\gamma_c(s)}=\frac{p\omega_{r_0}^2}{(s+p)\left(s^2+2\xi_0\omega_{r_0}s+\omega_{r_0}^2\right)}. \quad (32)$$

The variable $h$ is computed as below:

$$h=\dddot{\gamma}_d+k_2\ddot{e}+k_1\dot{e}=\dddot{\gamma}_d+k_2\left(\ddot{\gamma}_d-\ddot{\gamma}\right)+k_1\left(\dot{\gamma}_d-\dot{\gamma}\right), \quad (33)$$

$$\dddot{\gamma}_d=p\omega_{r_0}^2\left(\gamma_c-\gamma_d\right)-\left(\omega_{r_0}^2+2\xi_0\omega_{r_0}p\right)\dot{\gamma}_d-\left(p+2\xi_0\omega_{r_0}\right)\ddot{\gamma}_d. \quad (34)$$

The software implementation of the block diagram from Fig. 2 is provided in Fig. 3; for the numerical simulation, in order to validate the sliding mode control architecture, one considered the motion in vertical plane of a Vega rocket, some of the parameters associated to this kind of launch vehicle being presented in [24]; this is an expendable rocket developed by a team which includes the Italian Space Agency and the European Space Agency; the manufacturing work began in 1998 and the first launch was reported in 2012 from the Guiana Space Centre. Vega rocket launches small payloads (satellites), between 300 and 2500 kg, for scientific missions or for Earth observation. The values of the thrust force ($\boldsymbol{F}_c$)

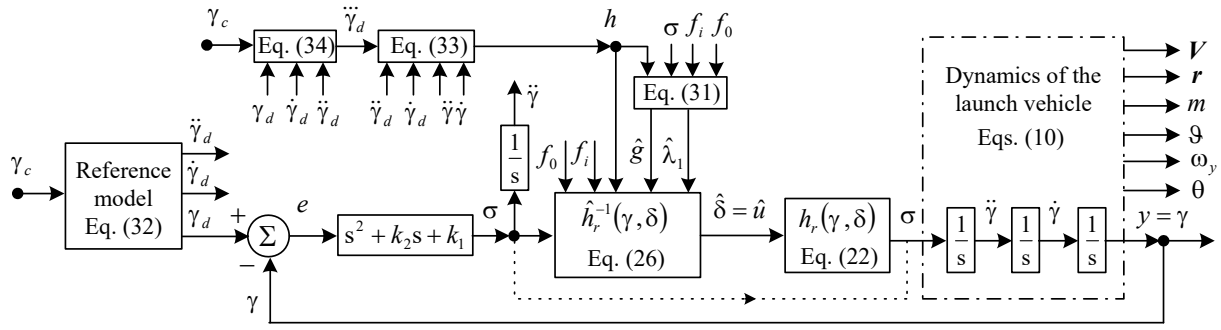


Fig. 2. Block diagram of the adaptive control system

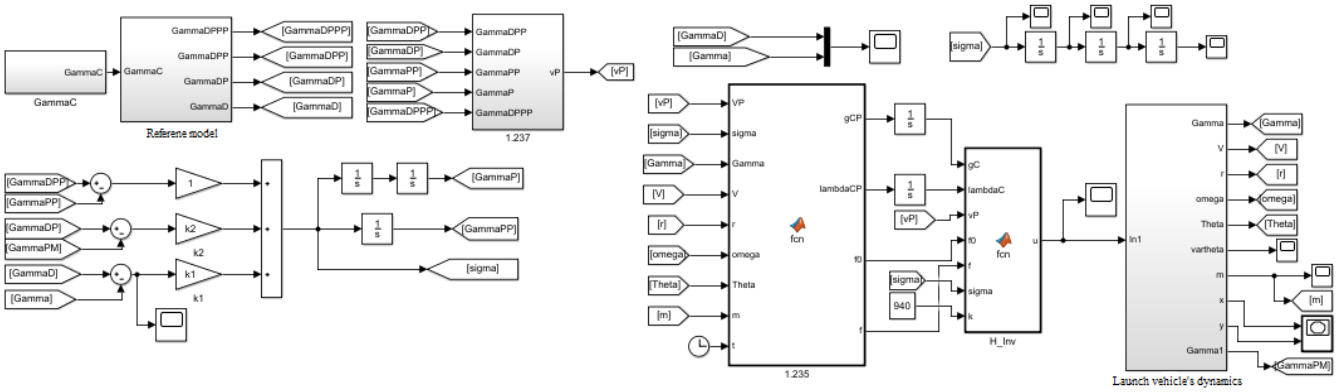


Fig. 3. Matlab/Simulink model for the system in Fig. 2

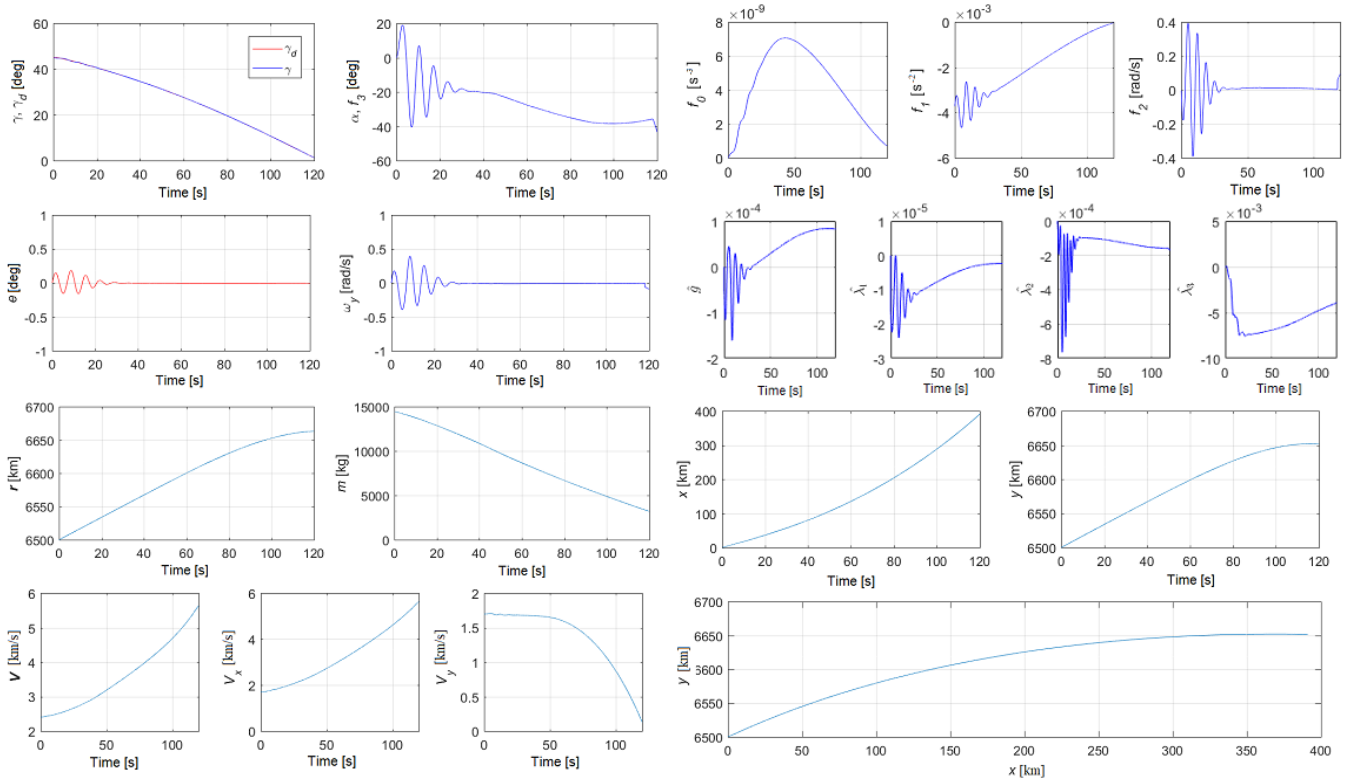


Fig. 4. Dynamic characteristics for the system in Fig. 2

depend on the time from the launch: $\boldsymbol{F}_c$=[180 260 290 330 300 260 240 200]*1000 [N] for time=[0 15 30 45 60 90 118 120] [s]. Aerodynamic coefficients $c_z^\alpha = c_y^\alpha$ depend on the Mach number; thus, for mach=[0 2 4 6 8 10 12 14], one obtained: $c_z^\alpha = c_y^\alpha$ =[0.9 1.5 1.6 1.8 2 2.3 2.5 2.9]. Inertia moment $J_{yy}$ is calculated as: $J_{yy} \cong \frac{m}{12}l^2 + \frac{m}{4}d^2$, where $l$=13.96 (the length of the rocket) and $d$=2.6 (the diameter of the rocket

principal section). Also, the following values have been chosen: $k = 44.5, k_1 = 2, k_2 = 4, \omega_{r_0} = 2$ rad/s, $\xi_0 = 0.7, p = 0.5$; the initial values of the most important variables are: $x(0) = 0\,\text{km}, y(0) = $ $= 6500\,\text{km}, V(0) = 2.4\,\text{km/s}, m(0) = 14457\,\text{kg}, \gamma(0) = 45\,\text{deg}$.

By dynamic inversion $\left(\hat{h}_r^{-1} h_r \cong 1\right)$, the system becomes linear and has on its direct way, closed by unitary negative feedback, the transfer function $H_d(\text{s}) = \dfrac{\text{s}^2 + k_2\text{s} + k_1}{\text{s}^3}$; the characteristic equation is $1 + H_d(\text{s}) = 0$, i.e.: $\text{s}^3 + \text{s}^2 + k_2\text{s} + k_1 = 0$; the coefficients $k_1$ and $k_2$ are computed such that the Hurwitz stability condition $k_2 > k_1 > 0$ is fulfilled. The time histories of main variables describing the motion of the launch vehicle in vertical plane are presented in Fig. 4.

The flight slope angle tracks the desired slope angle $\gamma_c$, with a very small error *e* which becomes null after 25 seconds. After about 120 seconds, $\gamma = \gamma_c \cong 0$ and, thus, according to Fig. 1, $V = V_x$ and $V_y = 0$ (horizontal displacement of the rocket, issue also confirmed by the characteristics of $V(t)$, $V_x(t)$, and $V_y(t)$); the force $\vec{F}_c$ forms an attack angle of $-40\,\text{deg}$, equal with the pitch angle $\theta$. Also, $y \to y_{\max} = r_{\max} = R_p + H_{\max} = $ $= 6650\,\text{km}$ and $x \to 400\,\text{km}$; the mass of the launch vehicle decreases from 15000 kg to about 3000 kg.

The new control architecture has the advantage of increased effectiveness compared to traditional approaches like PID having in mind that the behavior of the launch vehicle is changing continuously (the thrust force and moments of inertia are modified in the same time with the fuel consumption, change of aerodynamic parameters, location of the mass center and pressure center, dynamic pressure etc.); these changes have been taken into account in rocket's dynamics by its continuously update. As practical utility, the use of the proposed control architecture leads to improved flight safety and cost reduction.

## V. Conclusion

In this paper, one has designed an adaptive system for the control of the flight path slope angle in case of a launch vehicle during the second flight stage in vertical plane after the launching phase. By using a combination of the sliding mode control and dynamic inversion technique, one designed a control law depending on some estimated aerodynamics parameters. The equations of the estimated variables have been obtained from the condition that the system in closed loop is asymptotically stable (time derivative of the chosen Lyapunov function is negatively defined). The designed adaptive control system has been software implemented, tested, and validated through numerical simulations.

## References


[1] F.A. Butu, R. Lungu, and L.F. Barbulescu, "Adaptive flight control for a launch vehicle based on the concept of dynamic inversion," *20th International Conference on System Theory, Control and Computing*, 13-15 octombrie 2016.

[2] R. Su, Q. Zong, B. Tian, and M. You, "Comprehensive design of disturbance observer and non-singular terminal sliding mode control for reusable launch vehicles," *IET Control Theory Appl*. vol. 9, no. 12, 2015, pp. 1821.1830.

[3] Z. Wang, Z. Wu, and Y. Du, "Robust adaptive backstepping control for reentry reusable launch vehicles," *Acta Astronautica*, vol. 126, 2016, pp. 258-264.

[4] Y. Huang, C. Sun, C. Qian, and L. Wang, "Slow–fast loop gain-scheduled switching attitude tracking control for a near-space hypersonic vehicle," *Proc. Inst. Mech. Eng., Part I, J. Syst. Control Eng.*, vol. 227, no. 1, 2013, pp. 96-109.

[5] X. Shao and H. Wang, "Active disturbance rejection based trajectory linearization control for hypersonic reentry vehicle with bounded uncertainties," *ISA Transactions*, vol. 54, 2015, pp. 27-38.

[6] U. Ansari and A.H. Bajodah, "Generalized dynamic inversion scheme for satellite launch vehicle attitude control," *IFAC PapersOnLine* , vol. 48, no. 9, 2015, pp. 114-119.

[7] Q. Mao, L. Dou, Q. Zong, and Z. Ding, "Attitude controller design for reusable launch vehicles during reentry phase via compound adaptive fuzzy H-infinity control," *Aerospace Sciente and Technology*, vol. 72, 2018, pp. 36-48.

[8] F. Wang, C. Hua, Q. Zong, "Attitude control of reusable launch vehicle in reentry phase with input constraint via robust adaptive backstepping control," International Journal of Adaptive Control and Signal Process, vol. 29, no. 10, 2015, pp. 1308-1327.

[9] Y. Zhang, S. Tang, and J. Guo, "Adaptive-gain fast super-twisting sliding mode fault tolerant control for a reusable launch vehicle in reentry phase," *ISA Transactions*, vol. 71, 2017, pp. 380-390.

[10] H. Huang and Z. Zhang, "Characteristic model-based $H_2$/H-inf robust adaptive con-trol during the re-entry of hypersonic cruise vehicles," *Sci. China Inf. Sci.*, vol. 58, no. 1, 2015, pp. 1-21.

[11] H.F. Ghavidel and A. Kalat, "Robust control for mimo hybrid dynamical system of underwater vehicles by composite adaptive fuzzy estimation of uncertainties," *Nonlinear Dynamics*, 2017, pp. 1-19.

[12] M. Lungu, *Flight control systems (Sisteme de conducere a zborului)*, Sitech Publisher, Craiova, 2008.

[13] R. Lungu and M. Lungu, *Airplane automatic control during landing (Controlul automat al aeronavelor la aterizare)*, Sitech Publisher, 2015.

[14] E. Christopher and K. Sarah, *Sliding Mode Control: Theory and Applications*, Taylor & Francis International Ltd., 1998.

[15] S. Xingling and W. Honglun, "Sliding mode based trajectory linearization control for hypersonic reentry vehicle via extended disturbance observer," *ISA Transactions*, vol. 53, no. 6, 2015, pp. 1771-1786.

[16] Q. Zong, F. Wang, B. Tian, and R. Su, "Robust adaptive dynamic surface control design for a flexible air-breathing hypersonic vehicle with input constraints and uncertainty," *Nonlinear Dynamics*, vol. 78, no. 1, 2014, pp. 289-315.

[17] D.J. Bugajski and D.F. Enna, "Nonlinear Control Law with Application to High Angle of attack Flight," *Journal of Guidance, Control and Dynamics*, vol. 15, no. 3, 1992, pp. 761-777.

[18] H. Bouadi, H. Wu, and F. Mora-Camino, "Flight path tracking based-on direct adaptive sliding mode control," *IEEE Intelligent Vehicles Symposium,* 2011, pp. 25-30.

[19] F. Butu and R. Lungu, "Dynamics modeling and online identification of model parameters for a launch vehicle," *International Conference New Challenges in Aerospace Sciences*, Bucharest, 2015.

[20] M. Lungu, "Stabilization and control of a UAV flight attitude angles using the backstepping method," *World Academy of Science, Engineering and Technology*, vol. 6, no. 1, 2012, pp. 241-248.

[21] R. Lungu, M. Lungu, C. Rotaru, "Non-linear adaptive system for the control of the helicopters pitch's angle," *Proceedings of the Romanian Academy, Series A: Mathematics, Phisics, Technical Sciences, Information Science*, vol. 12, no. 2, 2011, pp. 133-142.

[22] M. Lungu and R. Lungu, "Reduced-Order Multiple Observer for Aircraft State Estimation during Landing," *Applied Mechanics and Materials*, vol. 841, 2016, pp. 253-259

[23] O. Harkergard and S.T. Glad, *A Backstepping Design for Flight Path Angle Control*, Sydney Publisher, Australia, 2000.

[24] E.C. Coskun, *Multistage Launch Vehicle Design with Thrust Profile and Trajectory Optimization*. PhD. Thesis, Middle East Tehnical University, Ankara, 2014.